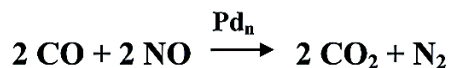
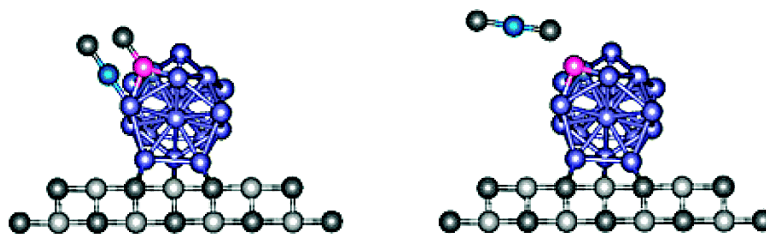


Cluster Size-Dependent Mechanisms of the CO + NO Reaction on Small Pd ($n \leq 30$) Clusters on Oxide Surfaces

Anke S. Wrz, Ken Judai, Stphane Abbet, and Ulrich Heiz

J. Am. Chem. Soc., **2003**, 125 (26), 7964-7970 • DOI: 10.1021/ja0352247 • Publication Date (Web): 10 June 2003

Downloaded from <http://pubs.acs.org> on March 29, 2009



More About This Article

Additional resources and features associated with this article are available within the HTML version:

- Supporting Information
- Links to the 10 articles that cite this article, as of the time of this article download
- Access to high resolution figures
- Links to articles and content related to this article
- Copyright permission to reproduce figures and/or text from this article

[View the Full Text HTML](#)



Cluster Size-Dependent Mechanisms of the CO + NO Reaction on Small Pd_n (n ≤ 30) Clusters on Oxide Surfaces

Anke S. Wörz, Ken Judai, Stéphane Abbet, and Ulrich Heiz*

Contribution from the University of Ulm, Institute of Surface Chemistry and Catalysis, Albert-Einstein-Allee 47, D-89069 Ulm, Germany

Received March 19, 2003; E-mail: ulrich.heiz@chemie.uni-ulm.de

Abstract: The CO + NO reaction ($2\text{CO} + 2\text{NO} \rightarrow \text{N}_2 + 2\text{CO}_2$) on small size-selected palladium clusters supported on thin MgO(100) films reveals distinct size effects in the size range Pd_n with $n \leq 30$. Clusters up to the tetramer are inert, while larger clusters form CO₂ at around 300 K, and this main reaction mechanism involves adsorbed CO and an adsorbed oxygen atom, a reaction product from the dissociation of NO. In addition, clusters consisting of 20–30 atoms reveal a low-temperature mechanism observed at temperatures below 150 K; the corresponding reaction mechanism can be described as a direct reaction of CO with molecularly adsorbed NO. Interestingly, for all reactive cluster sizes, the reaction temperature of the main mechanism is at least 150 K lower than those for palladium single crystals and larger particles. This indicates that the energetics of the reaction on clusters are distinctly different from those on bulklike systems. In the presented one-cycle experiments, the reaction is inhibited when strongly adsorbed NO blocks the CO adsorption sites. In addition, the obtained results reveal the interaction of NO with the clusters to show differences as a function of size; on larger clusters, both molecularly bonded and dissociated NO coexist, while on small clusters, NO is efficiently dissociated, and hardly any molecularly bonded NO is detected. The desorption of N₂ occurs on the reactive clusters between 300 and 500 K.

Introduction

During past decades, the NO + CO reaction has been studied in great detail, resulting in a tremendous number of studies, both experimental and theoretical (see refs 1–4 and references therein). The reason for this interest is mainly the aim to reduce air pollution. Nitrous oxides NO_x (NO, NO₂, etc.) are among other molecules such as O₂, CO, H₂, and hydrocarbons apparent in the exhaust gases from internal combustion engines. The apparent NO_x species need to be removed because they undergo photochemical reactions with hydrocarbons and oxygen and produce ozone in the atmosphere. To reduce the toxic properties from car exhaust, the first catalysts were manufactured at the beginning of the 1970's, and the first three-way catalysts (TWC) were built at the end of that decade. The idea of the TWC is to remove CO and NO_x and to oxidize unburnt hydrocarbons.^{1–3} Presently, the commercial catalysts contain rhodium as the active part for the reduction of NO to N₂ ($2\text{NO} + 2\text{CO} \rightarrow \text{N}_2 + 2\text{CO}_2$). Rh reduces NO with high efficiency, and it is so far the most active catalyst for the reaction. A number of experimental and theoretical studies revealed a detailed picture of the reaction mechanism.⁴ With this knowledge, one aims to find cheaper and more abundant metals instead of rhodium. Palladium is considered to be the most promising replacement. It is more durable at higher temperatures, and thus catalysts which contain Pd instead of Rh could be positioned closer to the engine.

The CO + NO reaction on Pd single crystals and supported particles has been investigated in detail, too.^{5–19} In short, the reaction is structure-sensitive, and the activity is increasing from more open surfaces to closed packed ones (Pd(100) < Pd(110) < Pd(111)).^{12,16,17} For supported Pd particles, the efficiency of the CO₂ formation changes with cluster sizes, and clusters with the highest density of closed packed facets are most active.^{7,8,16,18} It was found that adsorbed NO dissociates on the surface, resulting in two different types of adsorbed N_a with one type more strongly bound to the surface than the other. The more strongly bound N_a is poisoning the surface. To understand the structure-sensitivity, it is important to know that the relative concentration of poisoning N_a is decreasing from Pd(100) to

(1) Taylor, K. C. *Catal. Rev.-Sci. Eng.* **1993**, *35*, 457.
(2) Shelef, M.; Graham, G. W. *Catal. Rev.-Sci. Eng.* **1994**, *36*, 433.
(3) Nieuwenhuys, B. E. *Adv. Catal.* **1999**, *44*, 259.
(4) Zhdanov, V. P.; Kasemo, B. *Surf. Sci. Rep.* **1997**, *29*, 31.

(5) Daté, M.; Okuyama, H.; Takagi, N.; Nishijima, M.; Aruga, T. *Surf. Sci.* **1995**, *341*, L1096.
(6) Daté, M.; Okuyama, H.; Takagi, N.; Nishijima, M.; Aruga, T. *Surf. Sci.* **1996**, *350*, 79.
(7) Piccolo, L.; Henry, C. R. *Appl. Surf. Sci.* **2000**, *162–163*, 670.
(8) Piccolo, L.; Henry, C. R. *J. Mol. Catal. A* **2001**, *167*, 181.
(9) Pisanu, A. M.; Gigola, C. E. *Appl. Catal., B* **1999**, *20*, 179.
(10) Hirsimäki, M.; Suhonen, S.; Pere, J.; Valden, M.; Pessa, M. *Surf. Sci.* **1998**, *402–404*, 187.
(11) Rainer, D. R.; Koranne, M.; Vesecky, S. M.; Goodman, D. W. *J. Phys. Chem. B* **1997**, *101*, 10769.
(12) Vesecky, S. M.; Rainer, D. R.; Goodman, D. W. *J. Vac. Sci. Technol., A* **1996**, *14*, 1457.
(13) Muraki, H.; Fujitani, Y. *Ind. Eng. Chem. Prod. Res. Dev.* **1986**, *25*, 414.
(14) Muraki, H.; Shinjoh, H.; Fujitani, Y. *Ind. Eng. Chem. Prod. Res. Dev.* **1986**, *15*, 414.
(15) Xu, X.; Chen, P.; Goodman, D. W. *J. Phys. Chem. B* **1994**, *98*, 9242.
(16) Rainer, D. R.; Vesecky, S. M.; Koranne, M.; Oh, W. S.; Goodman, D. W. *J. Catal.* **1997**, *167*, 241.
(17) Vesecky, S. M.; Chen, P.; Xu, X.; Goodman, D. W. *J. Vac. Sci. Technol., A* **1995**, *13*, 1539.
(18) Xu, X.; Goodman, D. W. *Catal. Lett.* **1994**, *24*, 31.
(19) Honkala, K.; Piriälä, P.; Laasonen, K. *Surf. Sci.* **2001**, *489*, 72.

Pd(111).¹⁶ All of these studies dealt with nanometer-sized particles consisting of hundreds to thousands of atoms. Here, we present for the first time data of the mechanisms of the CO + NO reaction on small, size-selected supported Pd_n clusters with $n \leq 30$. This size range is of interest as cluster sizes are in the non-scalable regime; for example, quantum size effects become essential. The importance of these effects has been illustrated in past years by several studies,^{20–22} where the chemical reactivity was investigated on size-selected clusters supported on oxide surfaces. Surprisingly, the reaction mechanism of the CO + NO reaction is changing with size, and, most interestingly, the reaction temperatures are lower by at least 150 K on all palladium clusters in comparison to larger particles and single crystals under similar reaction conditions.

Experimental Methods

Clean Pd clusters are generated with a high-frequency laser evaporation source, producing high currents of singly and positively charged clusters. In this setup, the output (355 nm) of an Nd:Yag-laser is focused on a rotating Pd-target disk.²³ A helium pulse thermalizes the produced metal plasma, and the clusters are grown by nucleation when the helium-metal vapor undergoes supersonic expansion. Subsequently, they are size-selected by a quadrupole mass filter and deposited onto a magnesium oxide thin film. The total deposition energy is composed of the kinetic energy of the cluster ($E_{\text{kin}} < 0.2$ eV/atom), the chemical binding energy between the cluster and the MgO surface, as well as a negligible Coulomb interaction of the incoming cluster ion and its induced polarization charge on the oxide film surface. Consequently, as the kinetic energies of the impinging clusters correspond to soft-landing conditions ($E_{\text{kin}} \leq 1$ eV)^{24,25} and as the total energy gained upon deposition is smaller than the binding energy of the investigated clusters, cluster fragmentation is excluded. Upon impact, the cluster ions are neutralized by charge tunneling through the thin MgO films. We deposited only at most 0.3% of a monolayer cluster (1 ML = 2.25×10^{15} clusters/cm²) at 90 K to land them isolated on the surface and to prevent agglomeration on the MgO-films. In the Monte Carlo simulation, the relative number of isolated clusters was estimated to be higher than 95% after the clusters landed on the surface and migrated to the trapping centers.²⁶

The support is prepared in situ for each experiment by epitaxially growing thin films on a Mo(100) surface by evaporating magnesium in a ¹⁶O₂ background.²⁷ By changing the preparation method, for example, the Mg evaporation rate and the oxygen background, films with different defect densities can be prepared: defect-poor (Mg evaporation rate, 0.3–0.5 ML/min; O₂ background, 5×10^{-7} Torr) and defect-rich (Mg evaporation rate, 2–5 ML/min; O₂ background, 10^{-6} Torr) films. Both films are annealed to 840 K over 10 min. Auger electron spectroscopy (AES) measurements show a 1:1 stoichiometry for magnesium and oxygen and the absence of any impurity. Typical thicknesses are about 10 monolayers, as was determined by AES peak intensities and by X-ray photoemission (XPS), using the intensity attenuation of the Mo 3d core level with increasing film coverage. Both films have also been studied by electron energy loss spectroscopy. In

contrast to defect-poor films, which are characterized by a loss at about 6 eV in the EEL spectra (in good agreement with previous studies on MgO(100) single crystals), the EEL spectra of defect-rich films exhibit characteristic losses between 1 and 4 eV, lying within the MgO band gap. Similar loss structures have been observed before, and, according to first-principle calculations using large cluster models, they have been attributed to transitions characteristic for neutral surface F centers in various coordinations on flat terraces, at steps, and at kinks. The density of these oxygen vacancies is estimated to be larger than 5×10^{13} /cm².²⁸ In all of the experiments presented here, the clusters were deposited on defect-rich films to stabilize the clusters on these trapping centers.

To obtain identical conditions for the study of the chemical reactivity of the clusters, we first exposed the prepared model system by a calibrated molecular beam doser at 90 K to 1 Langmuir [$L = 1 \times 10^{-6}$ Torr s] of ¹³C¹⁶O. This results in saturation coverages on the clusters, as is evidenced by the desorption of physisorbed species from the oxide surface. Subsequently, we exposed the system to the same amount of ¹⁵N¹⁶O. This is crucial, as it is well known from single-crystal studies that the ratio of the reactants may influence the reactivity.^{10,17} Isotopically labeled ¹⁵N¹⁶O was used to distinguish the formation of N₂ from desorbing CO, both having a mass of 28 amu when using the naturally abundant isotope. In a temperature programmed reaction (TPR) experiment, we then detected the differently labeled CO₂ and N₂ molecules, which are produced on the surface of the clusters. The chemical reactivity is determined by integrating the TPR signal of the ¹³CO₂ and ¹⁵N₂ molecules and by normalizing to the number of deposited clusters. For this procedure, the mass spectrometer has been calibrated using the known amount of desorbing CO from a Mo(100) single crystal and taking into account its different sensibility for CO, CO₂, and N₂. The number of deposited clusters was obtained by integrating the measured ion current on the substrate over the deposition time. To distinguish the adsorption sites of the different molecules and to get additional information on the reaction mechanism, Fourier transform infrared spectroscopy (FTIR) is used.

Experimental Results

Clusters up to Pd₄ are inert with eventual ¹³CO₂ and ¹⁵N₂ peak heights comparable to the noise level of the TPR spectra; Pd_{5–7} produce a very small amount of CO₂, whereas larger clusters up to Pd₃₀ form CO₂ at around 300 K, with the temperature of maximal desorption rate slightly decreasing with cluster size (Figure 1a). Interestingly, additional formation and desorption of CO₂ is observed at around 140 K for Pd_n, with $n \geq 20$ (Figure 1a). This indicates that for these larger clusters two distinctly different reaction mechanisms occur. The formation of N₂ takes place between 300 and 500 K (Figure 1b). The normalized reactivities for the formation of CO₂ and N₂ per cluster are shown in the inserts of Figure 1 as a function of cluster size. For the CO₂ formation, only the main CO₂ desorption peak at around 300 K is considered. The reactivity is increasing when going from Pd₈ to larger clusters; for the measured cluster sizes, a local maximum is observed for Pd₁₅, whereas Pd₂₀ reveals a local reactivity minimum. For the formation of N₂, no clear critical cluster size is needed, and it increases nonmonotonically with cluster size. If the order of exposure is changed, that is, first NO and then CO, the formation of CO₂ is almost inhibited. Interestingly, the formation of N₂ is hardly altered for the larger clusters (Pd₃₀), whereas for smaller clusters (Pd₈), the N₂ signal is just above the noise level of the TPR spectra. This observation is illustrated for Pd₃₀ in Figure 2a/b and for Pd₈ in Figure 2c/d. The reason for this behavior becomes clear when analyzing the FTIR spectra taken for the

(20) Heiz, U.; Sanchez, A.; Abbet, S.; Schneider, W.-D. *J. Am. Chem. Soc.* **1999**, *121*, 3214.

(21) Häkkinen, H.; Abbet, S.; Sanchez, A.; Heiz, U.; Landman, U. *Angew. Chem., Int. Ed.* **2003**, *42*, 1297.

(22) Sanchez, A.; Abbet, S.; Heiz, U.; Schneider, W.-D.; Häkkinen, H.; Barnett, R. N.; Landman, U. *J. Phys. Chem. A* **1999**, *103*, 9573.

(23) Heiz, U.; Vanolli, F.; Trento, L.; Schneider, W.-D. *Rev. Sci. Instrum.* **1997**, *68*, 1986.

(24) Broman, K.; Félix, C.; Brune, H.; Harbich, W.; Monet, R.; Buttet, J.; Kern, K. *Science* **1996**, *274*, 956.

(25) Cheng, H.-P.; Landman, U. *J. Phys. Chem.* **1994**, *98*, 3527.

(26) Abbet, S.; Judai, K.; Klinger, L.; Heiz, U. *Pure Appl. Chem.* **2002**, *74*, 1527.

(27) Wu, M. C.; Estrada, C. A.; Goodman, D. W. *Phys. Rev. Lett.* **1991**, *67*, 2910.

(28) Heiz, U.; Schneider, W.-D. *J. Phys. D: Appl. Phys.* **2000**, *33*, R85.

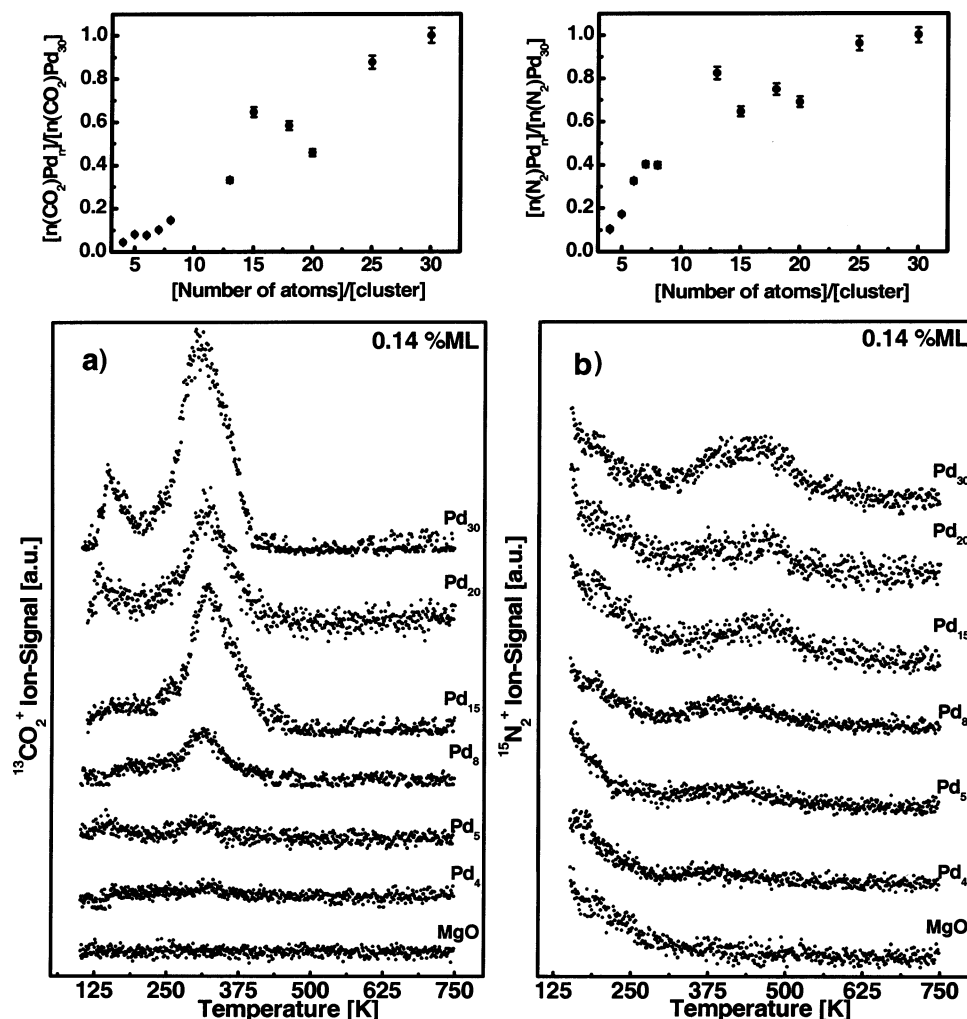


Figure 1. TPR-spectra of the reaction products $^{13}\text{CO}_2$ (Figure 1a) and $^{15}\text{N}_2$ (Figure 1b) as a function of cluster size. The cluster samples and a clean MgO film were first exposed at 90 K to ^{13}CO (1 L) and then to ^{15}NO (1 L). The reactivities expressed as the number of product molecules formed per cluster and normalized to the reactivity of Pd₃₀ are shown in the inserts for $^{13}\text{CO}_2$ and $^{15}\text{N}_2$. For the CO_2 desorption, only the main desorption peak at around 300 K is considered. We deposited between 0.14% ML and 0.31% ML of the size-selected clusters. We changed the coverage as a function of cluster size to approximately cover the same surface area. Note that the shown spectra are all scaled to 0.14% ML, resulting in different noise levels.

two different experimental conditions, shown for Pd₃₀ and Pd₈ in Figure 3 as a function of temperature. First, all spectra show absorption bands for NO and CO on the MgO film (^{13}CO , 2130 cm^{-1} ; ^{15}NO , 1830–1840 cm^{-1}), and these species are remaining on the surface up to temperatures of around 150 K. These bands are not discussed further. When the reaction takes place, that is, CO was dosed before NO, the FTIR spectra for both cluster sizes, Pd₃₀ (Figure 3a) and Pd₈ (Figure 3c), reveal intense absorption bands at around 2050 cm^{-1} (^{12}CO , 2097 cm^{-1}), typical for on-top-bonded CO. Note also that this band shifts toward lower frequency during reaction (increasing temperature). Additionally and most pronounced for Pd₃₀, an absorption band at 1930 cm^{-1} (^{12}CO , 1974 cm^{-1}) is detected. This band is typical for bridge-bonded CO. These assignments are supported by single-crystal studies where CO adsorbed on-top on Pd(111) reveals a band at around 2110 cm^{-1} , and the band at 1960–1970 cm^{-1} is attributed to bridge-bonded CO.²⁹ Under these experimental conditions, a small ^{15}NO absorption band at 1550 cm^{-1} (^{14}NO , 1578 cm^{-1}) is observed for Pd₃₀, only. Most of the nitric oxide is dissociated on the clusters prior to reaction.

This information is obtained from TPR studies of NO on clean and CO-covered Pd_n clusters, where, in both cases, the formation of N₂ is observed between 300 and 500 K. Thus, both reactants coexist on the cluster surface in molecular or dissociated form, and the reaction can occur via a Langmuir–Hinshelwood reaction mechanism. The FTIR spectra change completely when the clusters are first exposed to NO. For Pd₃₀, the main absorption is observed at 1720 cm^{-1} (^{14}NO , 1751 cm^{-1}) and is attributed to on-top-bound NO; at higher temperatures, the intensity of this absorption band decreases, and a new band appears at 1620 cm^{-1} (^{14}NO , 1649 cm^{-1}). These vibrational frequencies are comparable to those of molecularly bound NO on single crystals.¹⁵ For Pd(111), a band at around 1750 cm^{-1} is attributed to on-top-bound NO, whereas bands at ~ 1530 cm^{-1} and ~ 1580 cm^{-1} are typical for two- and three-fold-bound species. On the stepped surface Pd(112) and at elevated temperature, an absorption is observed between 1655–1670 cm^{-1} ,³⁰ whereas at high coverage, bridge-bound NO on Pd(100) gives rise to an absorption band between 1630–1670 cm^{-1} .¹⁵ TPR experiments reveal that also dissociated NO is present on

(29) Tüshaus, M.; Berndt, W.; Conrad, H.; Bradshaw, A. M.; Persson, B. *Appl. Phys. A* **1990**, *51*, 91.

(30) Ramsier, R. D.; Gao, Q.; Neergaard Waltenburg, H.; Lee, K. W.; Nooij, O. W.; Lefferts, L.; Yates, J. T. *J. Surf. Sci.* **1994**, *320*, 209.

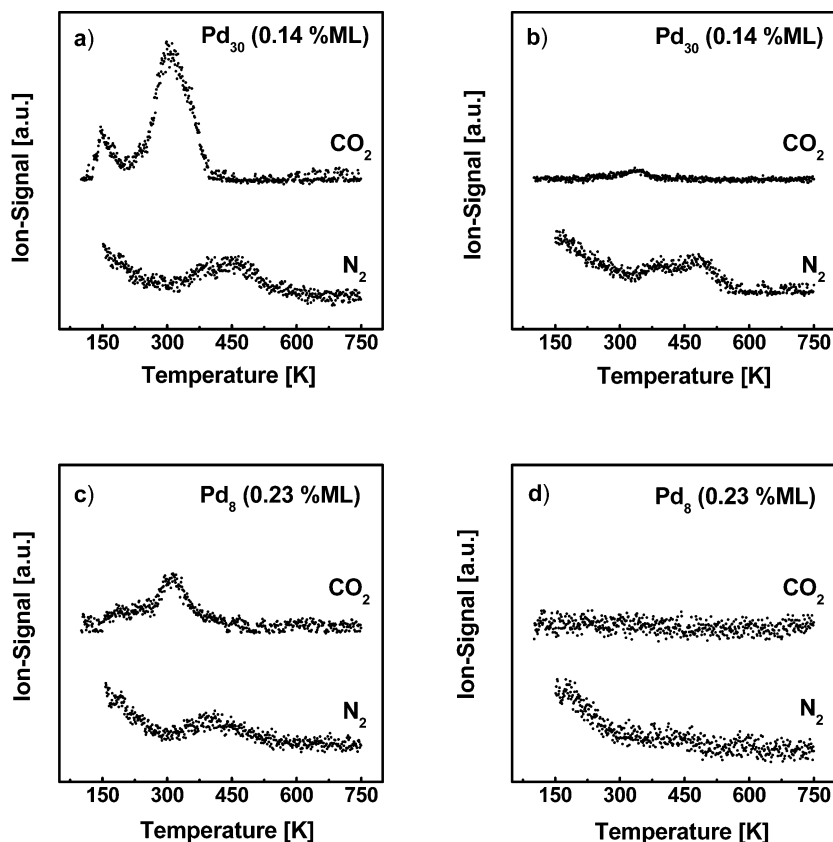


Figure 2. The importance of the order of gas exposure. Figure 2a/c shows the desorption spectra for $^{13}\text{CO}_2$ and $^{15}\text{N}_2$ if ^{13}CO is dosed in the first step and ^{15}NO is dosed subsequently. Figure 2b/d shows the TPR-spectra if ^{15}NO was exposed in the first step.

the cluster surface as N_2 starts to desorb at around 300 K (Figure 2b). The intensity of the CO absorption band at 2075 cm^{-1} (^{12}CO , 2122 cm^{-1}) decreases drastically and explains the small formation of CO_2 under these experimental conditions (Figure 3b/d). Interestingly and consistent with the observation that no CO_2 is formed on Pd_8 (Figure 2d), the absorption band of CO observed for this cluster size is considerably smaller (Figure 3d). Furthermore, the absorption band of molecularly adsorbed NO at around 1700 cm^{-1} (^{14}NO , 1731 cm^{-1}) is almost absent (Figure 3d), indicating that this cluster size efficiently dissociates NO. This difference in the interaction of NO with small (Pd_8) and large (Pd_{30}) clusters was also observed without coadsorption of CO. Pd_{30} reveals an absorption band of molecularly bound NO, and the desorption of NO and N_2 is detected by TPR, whereas on Pd_8 hardly any molecular-bound NO can be detected (not shown here).

As mentioned above, the low-temperature formation of CO_2 at temperatures lower than 150 K is observed exclusively for Pd_n , with $n \geq 20$ (Figure 1a). A closer comparison of the IR-spectra of Pd_{30} (Figure 3a) and Pd_8 (Figure 3c) is clarifying, as at low temperature an absorption band at around 1550 cm^{-1} (^{14}NO , 1578 cm^{-1}) is observed reproducibly for Pd_{30} only. If we compare these results with those from single-crystal experiments, this band can be attributed to three-fold-bound NO.¹⁵ In concert with the low-temperature formation of CO_2 observed for this cluster size, this band disappears at around 160 K, indicating that for the low-temperature mechanism a molecular, three-fold-bonded NO may be involved. The nonappearance of this band for Pd_8 is in agreement with the absence of this mechanism for this cluster size. To ensure that molecular NO is indeed involved in the low-temperature mechanism, we

performed the following experiment. Pd_{30} was exposed to NO at 90 K, and the cluster sample was then annealed to 350 K; at this temperature, molecularly bonded NO completely desorbs from the cluster, as is evidenced by FTIR and TPR, but the dissociation products of NO, which are O_a and N_a , are still present on the surface (the formation of N_2 is observed between 300 and 500 K). Subsequently, the sample was cooled to 90 K and was exposed to CO. The resulting TPR spectrum indeed shows that the low-temperature formation of CO_2 is absent (Figure 4a). The formation of CO_2 at higher temperature, however, indicates that, in contrast to molecularly adsorbed NO, O_a and N_a do not inhibit the coadsorption of CO. The same is true for Pd_8 , as is evidenced by the results shown in Figure 4b. In summary, these experiments clearly identify the intermediates of the two reaction mechanisms. At low temperature, molecular NO reacts with adsorbed CO to form CO_2 , whereas at high temperature the CO molecules are oxidized by adsorbed oxygen atoms originating from the NO-dissociation on the cluster. In addition, under NO-rich conditions, CO-adsorption is inhibited by molecularly adsorbed NO.

Discussion

The results presented here extend the studies on the structure-sensitivity of the CO + NO reaction on palladium down to the atom. For single crystals, the reactivity is decreasing going from the closed packed Pd(111) surface to the more open surfaces. Two reasons are responsible for this observation. First, the relative NO concentration in comparison to CO is higher on Pd(111) than on Pd(100).¹⁷ Second, the more open surfaces, like Pd(100), are poisoned by strongly adsorbed nitrogen atoms, N_a . In detail, NO dissociates on the surface, leading to two

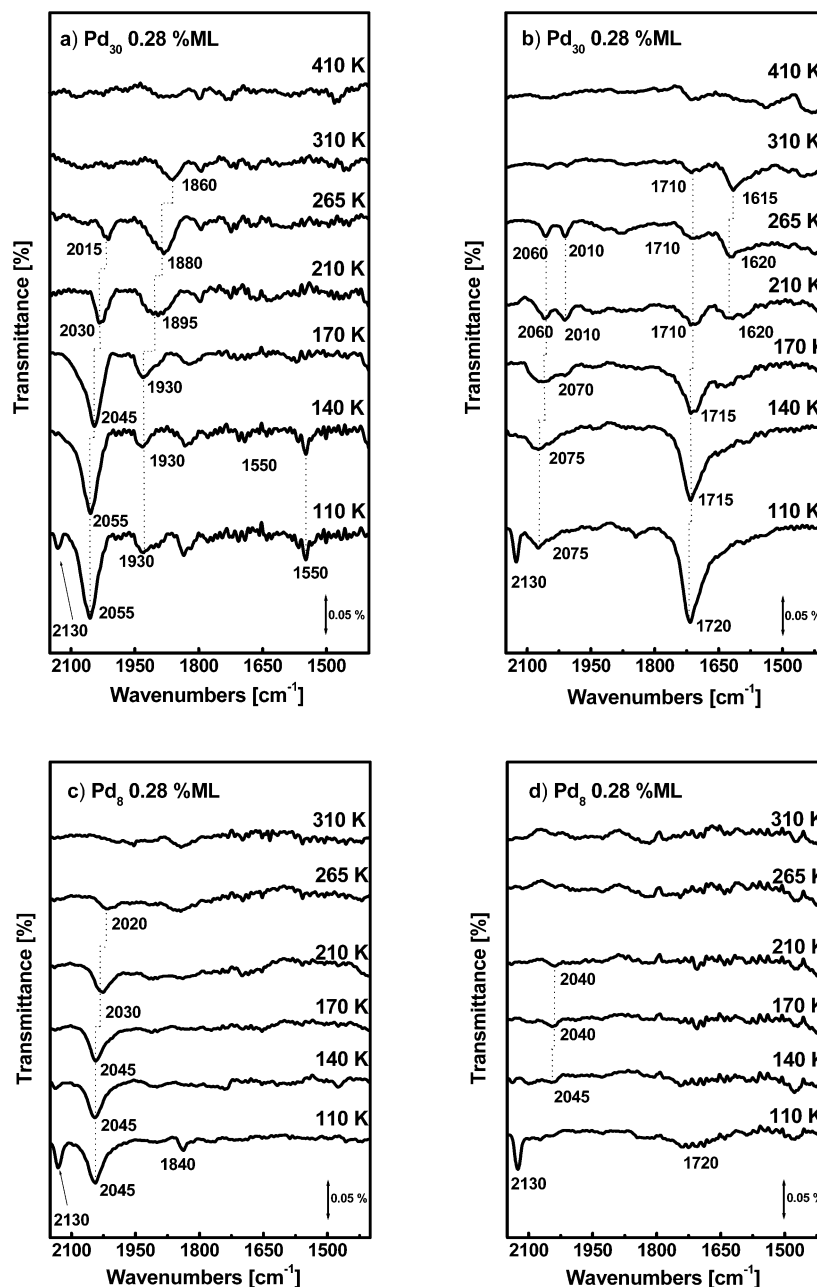


Figure 3. IR-spectra of ^{13}CO and ^{15}NO adsorbed on Pd_{30} (Figure 3a/b) and Pd_8 (Figure 3c/d) clusters. Figure 3a/c shows the spectra if ^{13}CO was preadsorbed for both cluster sizes. Figure 3b/d shows the spectra if ^{15}NO was preadsorbed. All of the spectra were taken at 90 K after annealing the cluster samples to the indicated temperatures.

different types of adsorbed nitrogen atoms, N_a . One is weakly bound to the surface, while for the other the bond energy is considerably larger. Corresponding thermal desorption experiments lead to two different desorption temperatures at ~ 450 – 480 K and ~ 520 – 600 K. The more strongly adsorbed N_a is poisoning the surface. The relative amount of the strongly bound N_a is increasing from $\text{Pd}(111)$ to the more open surfaces.¹⁶

For particles with sizes larger than 25 \AA , the catalytic activity for the $\text{CO} + \text{NO}$ reaction is increasing with particle size as the relative amount of the more reactive $\text{Pd}(111)$ facets is increasing. In addition, smaller particles reveal a higher density of low coordinated adsorption sites, leading to more efficient dissociation of NO and strongly adsorbed nitrogen atoms.¹⁶

For even smaller palladium particles in the size range from 2.7 to 15.6 nm and supported on MgO surfaces, a maximum in

reactivity is observed for the mid-sized particles (6.9 nm).⁸ For understanding these size effects, concepts from single crystal studies were applied, too. Mid-sized particles consist mainly of $\text{Pd}(111)$ facets, while the larger cluster exposes a high density of $\text{Pd}(100)$ facets, which originate from coalescence. Although the small particles reveal $\text{Pd}(111)$ facets, the density of low-coordinated Pd atoms (steps and kinks) is increased, and thus the dissociation of NO and the amount of strongly adsorbed N_a is higher.^{8,31} In addition, for these particles, the rate-limiting step for the reaction is changing with temperature.⁸ At low temperatures, the NO dissociation is rate-limiting, while at high temperature, the CO adsorption is rate-limiting.

(31) Giorgio, S.; Henry, C. R.; Chapon, C.; Penisson, J. M. *J. Cryst. Growth* **1990**, *100*, 254.

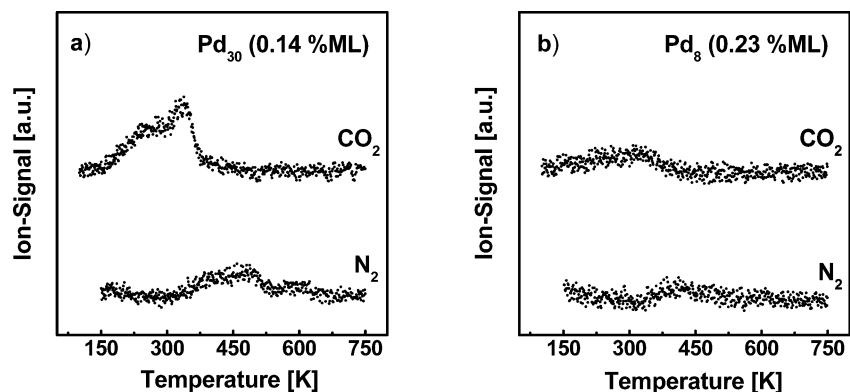


Figure 4. TPR results of an experiment in which Pd₃₀ (a) and Pd₈ (b) were first exposed to ¹⁵NO and subsequently annealed up to around 350 K. After the samples were cooled to 90 K, they were exposed to ¹³CO, and the resulting product molecules were monitored by TPR.

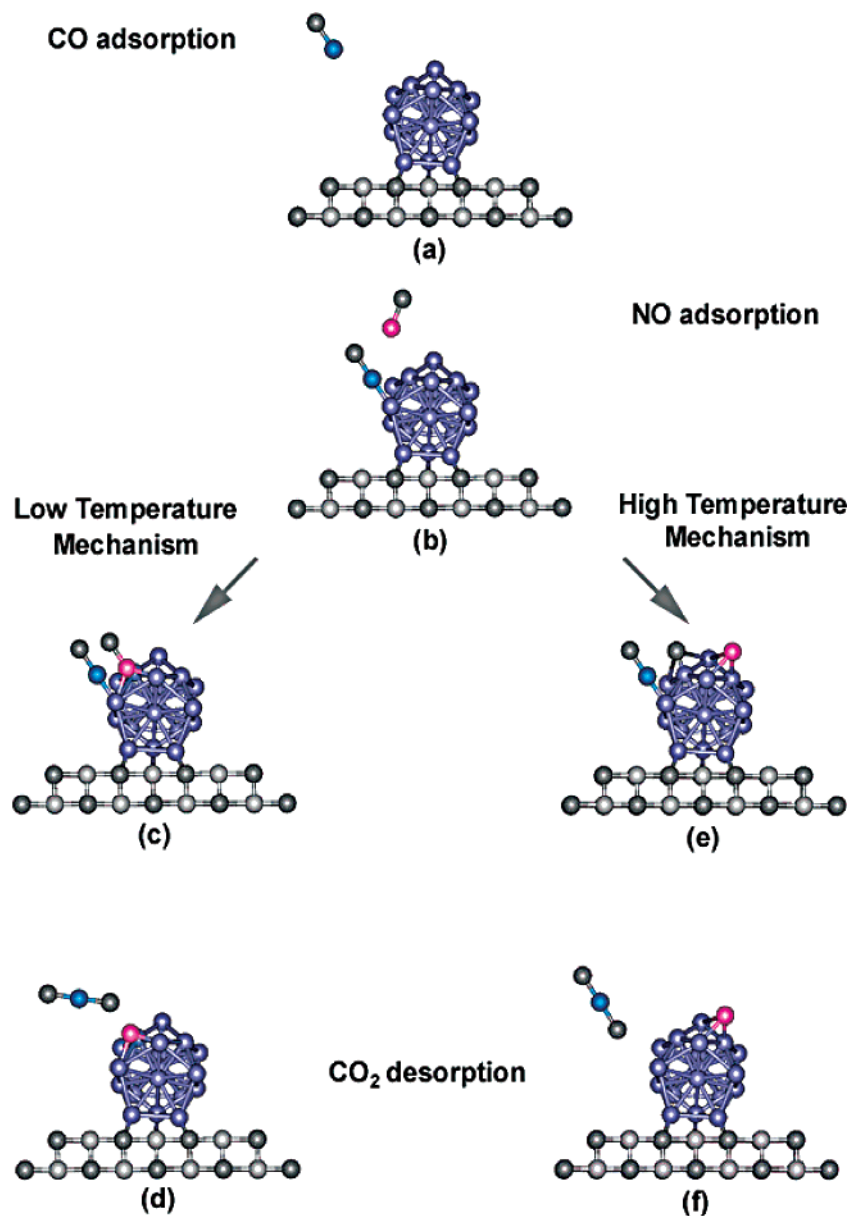


Figure 5. Schematically shown are the two possible reaction paths for the low-temperature formation of CO₂ with the adsorption of the reactants CO (Figure 5a) and NO (Figure 5b) and the formation of CO₂ (Figure 5c/d) by direct reaction of CO_a and NO_a, as well as the high-temperature reaction path with CO_a and O_a (Figure 5e/f) as intermediates.

In this work, we extended the investigation of the structure-sensitivity of the CO + NO reaction on palladium to the very

small clusters consisting of up to a couple of dozens of atoms. In this size range, concepts from single-crystal studies fail as

first “nanocatalytic” concepts are involved,^{21,22} and second facets typical for single crystals do not exist. Indeed, in comparison to single crystals and Pd particles,^{5,8,11,16,18} two important differences are observed for these cluster model catalysts. First, the low-temperature mechanism at around 140 K has not yet been observed, and second the main mechanism on all clusters occurs at temperatures at least 150 K lower than for particles or single crystals. The low-temperature reaction mechanism is observed for Pd_n with $n \geq 20$, only. Combined FTIR and TPR studies show that CO directly reacts with molecularly adsorbed NO, bound at the larger clusters at three-fold binding sites; in these cases, NO is activated and reacts directly with CO. Down to Pd₅, CO₂ is formed at around 300 K under CO-rich conditions. As for larger particles and single crystals, the reaction mechanism involves molecularly adsorbed CO and O_a from the dissociation of NO at the cluster. The two different reaction mechanisms are illustrated schematically in Figure 5. Surprisingly, for all investigated cluster sizes, the reaction takes place at low temperatures (freezing temperature), while for the reaction on single crystals and nanometer-sized particles, higher temperatures are necessary. In the case of Pd single crystals and larger particles, the formation/desorption temperature of the produced CO₂ is between 450 and 600 K.^{5–7,10,18} The reason for this surprising effect is not yet understood; one reason may be the impossibility of migration of oxygen atoms into the cluster, and thus the involved activation energies are largely decreased. On going to even smaller clusters consisting of up to four atoms, the reaction is completely suppressed, as these small clusters cannot accommodate a sufficient number of reactant molecules.

Conclusion

The efficiency of the CO + NO reaction on size-selected Pd_n clusters supported on MgO thin films is strongly size-dependent. Whereas palladium clusters up to the tetramer are inert, clusters up to Pd₁₉ show reactivity at 300 K only. Larger clusters are reactive at temperatures as low as 140 K. The high-temperature reaction mechanism is described by the oxidation of CO by adsorbed oxygen atoms, whereas in the low-temperature mechanism CO directly reacts with molecularly adsorbed NO. The efficiency of the reaction increases non-monotonically with cluster size, revealing a local maximum for Pd₁₅, whereas a local minimum is observed for Pd₂₀. Most importantly, the reaction temperature of the main reaction mechanism is at least 150 K smaller than those for larger particles and single crystals.

Acknowledgment. This work was supported by the Deutsche Forschungsgemeinschaft. A.S.W. acknowledges support from the Graduiertenkolleg “Molekulare Organization und Dynamik an Grenz- und Oberflächen”, K.J. thanks the Alexander v. Humboldt foundation and the Japan Society for the Promotion of Science (JSPS) foundation for financial support, and S.A. thanks the Swiss National Science foundation and the Alexander v. Humboldt foundation for financial support.

Supporting Information Available: FTIR spectra (PDF). This material is available free of charge via the Internet at <http://pubs.acs.org>.

JA0352247